

Stark effect in dye-doped polymers studied by photochemically accumulated photon echo

Hansruedi Gygax, Alexander Rebane, and Urs P. Wild

Physical Chemistry Laboratory, Swiss Federal Institute of Technology, ETH-Zentrum, CH-8092 Zurich, Switzerland

Received October 6, 1992; revised manuscript received January 21, 1993

We study theoretically and experimentally the influence of a homogeneous static electric field on a photochemically accumulated stimulated photon echo in dye-doped polymers. The dependence of the time profile of the echo signal on the strength of the electric field is evaluated in the case of a linear Stark effect. Experiments using polymers doped with organic dye molecules are carried out at low temperature, and our new technique is applied to determine the difference of the permanent dipole moment in the ground and the first excited singlet electronic state of the impurity molecules.

INTRODUCTION

Narrow zero-phonon lines^{1,2} (ZPL's) are sensitive probes for studying the effect of external and internal electric fields on impurity molecules in solids. With organic impurity molecules doped into polymers, one can produce, by moderate applied field strengths, Stark shifts that are orders of magnitude larger than the homogeneous width of ZPL's at liquid-helium temperatures ($\Gamma_{\text{hom}} \sim 10^{-2} - 10^{-3} \text{ cm}^{-1}$). On the other hand, the inhomogeneous broadening of ZPL's in organic polymers is remarkably large ($\Delta\nu_{\text{inhom}} \sim 10^2 \text{ cm}^{-1}$), so that the Stark shifts of ZPL's are completely obscured by inhomogeneous broadening of the spectra. Several methods based on persistent spectral hole burning^{3,4} (PSHB) and the application of narrowband tunable lasers for excitation,⁵⁻⁷ as well as using the technique of holographic detection of narrow spectral holes,^{8,9} have been developed to avoid the inhomogeneous broadening of spectra and to study the Stark effect in polymers.

An alternative approach to eliminating the inhomogeneous broadening of ZPL's is by time-domain coherent optical phenomena such as photon echo¹⁰ and, especially in PSHB media, the method of photochemically accumulated stimulated photon echo (PASPE).^{11,12} PASPE results from scattering (diffraction) of a probe pulse from a frequency-domain grating that has previously been written in the inhomogeneous frequency distribution of the ZPL's by illumination with sequences of coherent pulses.^{11,13} The origin of PASPE is similar to the phenomena of stimulated photon echoes^{14,15} and to the photon echoes observed from transient spectral gratings because of population accumulation in the triplet bottleneck.¹⁶ The distinctive feature of PASPE is a practically infinite lifetime of the bottleneck state, actually given by the very long lifetime (hours, days) of the photoproduct state. The amplitude of PASPE is given by the Fourier transform of the shape of the grating in the frequency domain (at least so long as the scattering process is treated in linear terms¹⁷) and relates to the homogeneous line shape.

It is apparent that, if the Stark effect shifts the frequency of ZPL's, then it should also influence the coherent time-domain response of the media and facilitate, as a

consequence, the determination of the Stark effect parameters of the impurity center. In addition, because the PASPE technique has several potential applications in time-domain holographic processing of ultrashort optical signals,^{18,19} the effect of an external field on time-domain holograms must be investigated.

We have previously reported²⁰ that an external electric field alters the intensity of PASPE. At liquid-helium temperature, PASPE signals were accumulated in a polyvinylbutyral (PVB) film doped with chlorin molecules, and during the readout an electric field was applied. When we increased the voltage applied across the sample, the intensity of the echo signal first decreased from its initial absolute maximum value to zero and then increased again when the voltage was further increased. The sensitivity of the echo signal to the applied Stark field was dependent on the time delay between the picosecond pulses used to write the frequency-domain grating, and the echo signal did not vanish only if the delay was made equal to zero. Reference 20 gives a qualitative explanation of the observed phenomena in terms of a set of spectral holes that constitute the grating: if the spectral profile of one narrow hole splits and broadens in the Stark field, then at a certain value of the splitting the contrast in the spectral domain vanishes, and so also does the intensity of the echo signal. When the Stark splitting of the holes is further increased, the contrast in the spectral domain increases again and the PASPE signal reappears. The lack of sensitivity to the electric field at zero delay is due simply to the absence of a frequency-domain grating: only a spatial grating exists.

To evaluate the behavior of the PASPE signal in an external field on a quantitative level, we need to consider how the Stark effect alters the resonance frequencies of ZPL's within the inhomogeneously broadened band. The time profile of the coherent response is then given by the Fourier transform of the altered ZPL frequency distribution function.

Recently a modulation of the photon-echo intensity as a function of an applied electric field was observed also in a crystalline system of Eu^{3+} in YAlO_3 .^{21,22} On a qualitative level, the explanation of this phenomenon is similar to that

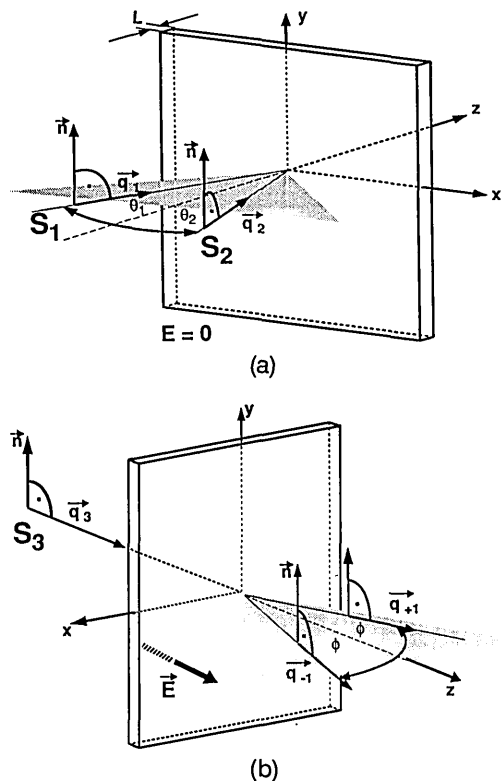


Fig. 1. (a) Geometry of the writing procedure. The PSHB plate is positioned in the plane $z = 0$. Propagation vectors of the writing beams \mathbf{q}_1 and \mathbf{q}_2 are in the (x, z) plane. The polarization vectors are parallel to the y axis. The value of the applied electric field is zero. (b) Geometry of the read procedure. The probe beam propagates in the direction of the z axis and is polarized parallel to the y axis. The external electric field \mathbf{E} is applied perpendicular to the plane of the PSHB plate parallel to the z axis.

given above. The differences between the two experiments come from much larger inhomogeneous and homogeneous linewidths of polymeric systems compared with those of crystals and from the random orientation of the dye molecules in polymeric matrices versus the orientational order of the impurity centers in a crystalline environment.

In this paper we derive general formulas that describe the dependence of the time profile of an arbitrary PASPE signal on the external electric field. Numerical results are presented for the case of linear Stark effect for impurity molecules with intrinsic- and matrix-induced permanent dipole moments. We also carry out experiments with PVB film doped with molecules of chlorin and octaethylporphyrin and compare the results of our model calculations with the experimental data.

THEORY

In this section we evaluate the general formulas that describe the dependence of the amplitude of PASPE on the homogeneous external electric field applied during the readout of the spectral grating. During the writing stage of the PSHB spectral grating the external electric field is zero.

Consider two plane-wave laser pulses of complex envelopes $s_1(t)$ and $s_2(t)$ with the spectrum centered around the optical carrier frequency ν_0 . Let the pulses illumi-

nate successively a thin polymer film of thickness L doped with dye molecules that are subject to PSHB [see Fig. 1(a)]. The film is positioned at plane $z = 0$ of the coordinate system, the illuminating pulses propagate toward the PSHB recording medium in the positive z -axis direction at angles Θ_1 and Θ_2 in the (x, y) plane, which are close to the normal incidence of the film. The polarization of the pulses is assumed to be linear; the electric component points in the direction of the y axis. The oscillating electric field incident upon the polymer film is given by

$$\mathbf{A}(t, \mathbf{r}) = \mathbf{n} \left\{ s_1 \left(t - \frac{\mathbf{q}_1 \mathbf{r}}{c} \right) \exp \left[i 2 \pi \nu_0 \left(t - \frac{\mathbf{q}_1 \mathbf{r}}{c} \right) \right] + s_2 \left(t - \frac{\mathbf{q}_2 \mathbf{r}}{c} - \tau \right) \exp \left[i 2 \pi \nu_0 \left(t - \frac{\mathbf{q}_2 \mathbf{r}}{c} - \tau \right) \right] \right\}, \quad (1)$$

where $\mathbf{q}_1 = (\sin \Theta_1, 0, \cos \Theta_1)$ and $\mathbf{q}_2 = (-\sin \Theta_2, 0, \cos \Theta_2)$, τ is the time delay between the pulses at the point of the origin ($\mathbf{r} = 0$), \mathbf{n} is the unit polarization vector, and c is the speed of light. We present the amplitude of the pulses by their Fourier transforms,

$$s(t) = \hat{F}^{-1}(\tilde{s}(\omega)) = \frac{1}{2\pi} \int_{-\infty}^{\infty} \tilde{s}(\omega) \exp(i\omega t) d\omega, \quad (2)$$

and express the intensity of light absorbed by the molecules of certain ZPL frequency at coordinate x through the absolute square of the sum of the Fourier amplitudes:

$$I(\omega, x) = |\tilde{s}_1(\omega - 2\pi\nu_0)|^2 + |\tilde{s}_2(\omega - 2\pi\nu_0)|^2 + \tilde{s}_2(\omega - 2\pi\nu_0) \tilde{s}_1^*(\omega - 2\pi\nu_0) \times \exp \left[i\omega \left(-\tau + \frac{x \sin \Phi}{c} \right) \right] + \tilde{s}_1(\omega - 2\pi\nu_0) \times \tilde{s}_2^*(\omega - 2\pi\nu_0) \exp \left[i\omega \left(\tau - \frac{x \sin \Phi}{c} \right) \right], \quad (3)$$

where $\sin \Phi = \sin \Theta_1 + \sin \Theta_2$ and where $*$ denotes the complex conjugate.

The inhomogeneous distribution function, $N(\omega, \Omega)$, gives the number of impurity molecules per unit volume, per frequency interval $\Delta\omega$, per unit solid angle, that have the ZPL in the frequency interval $(\omega, \omega + \Delta\omega)$ and are oriented with the transition dipole moment vector, \mathbf{d} , pointing along unit vector Ω .

Here we assume a one-photon PSHB process in which the photoproduct does not absorb at the wavelength of the original inhomogeneous absorption band. If the amplitude of the incident light is sufficiently low¹⁷ and satisfies the condition

$$|A(t)| \ll \frac{h\Gamma_{\text{hom}}}{|\mathbf{d}|}, \quad (4)$$

where h is Planck's constant, then the number of burned-out molecules is linearly proportional to the number of absorbed photons. To achieve an appreciable contrast of the spectral grating under the weak excitation condition (4), we assume that the illumination is repeated (accumulated) many times while the interval between the illumination cycles are kept longer than the relaxation time of the

impurity excited electronic state (typically 10^{-8} s). The variation of the inhomogeneous distribution function caused by the illumination is

$$\Delta N(\omega, x, \Omega) = -\eta \frac{(\mathbf{d}\mathbf{n})^2}{d^2} N^\circ(\omega, x, \Omega) [I(\omega, x) \otimes \Gamma(\omega)], \quad (5)$$

where N° is the chromophore concentration before illumination, $\Gamma(\omega)$ is the homogeneous ZPL line-shape function, and \otimes denotes integral operation of a convolution. The constant η is proportional to the quantum yield of the PSHB process, to the absorption cross-section of the ZPL's, and to the number of the accumulated pulse pairs. Here we assume that the summary illumination dose is small so that the number of the remaining impurity molecules is much larger than the number of bleached out molecules.

In a nonilluminated sample the transition dipole moments of the impurity molecules are isotropically oriented. We assume that before illumination the frequencies of ZPL's are statistically independent from the

perposition of the molecular oscillator responses to the probe pulse. The amplitude of the induced oscillations of a molecular dipole depends on the detuning between the frequency of the driving optical field and the ZPL resonance frequency. The ZPL resonance frequency experiences a shift in an external electric field, and the new value of the frequency detuning is

$$\omega' = 2\pi\nu_0 - [2\pi\nu_{\text{ZPL}} + F(\mathbf{E}, \Omega)], \quad (7)$$

where the Stark shift F depends on the orientation of the impurity molecule with respect to the vector of the applied static field. (We assume that the external field does not change the orientation of the dye molecules.)

We consider the probe beam to be linearly polarized along the y axis and to propagate perpendicular to the PSHB film in the direction of the z axis [Fig. 1(b)]. The amplitude polarized along the y axis immediately behind the PSHB film is expressed by summing the responses of the impurity molecules with different resonance frequencies and orientations^{17,18,23,24}:

$$\begin{aligned} A'(t, x, \mathbf{E}) &= \hat{F}^{-1} \left(\tilde{s}_3(\omega) \exp \left\{ -\frac{(2\pi)^2 \nu_0 L}{hc} \left\langle \frac{(\mathbf{d}\mathbf{n})^2 N'(\omega', \Omega, x)}{i[\omega' - \omega + F(\mathbf{E}, \Omega)] + \pi\Gamma_{\text{hom}}} \right\rangle \right\} \right) \\ &= \hat{F}^{-1} \left(\exp \left\{ -\alpha_0 \left\langle \frac{(\mathbf{d}\mathbf{n})^2}{i[\omega' - \omega + F(\mathbf{E}, \Omega)] + \pi\Gamma_{\text{hom}}} \right\rangle \right\} \tilde{s}_3(\omega) \left\{ 1 + \alpha_0 \left\langle \frac{(\mathbf{d}\mathbf{n})^4 [I(\omega', x) \otimes \Gamma(\omega')]}{i[\omega' - \omega + F(\mathbf{E}, \Omega)] + \pi\Gamma_{\text{hom}}} \right\rangle \right\} \right), \quad (8) \end{aligned}$$

orientation of the molecules and that the concentration of the impurity molecules is spatially homogeneous. For simplicity we assume also that the spectral width of the pulses is much less than the width of the inhomogeneous absorption band. The inhomogeneous distribution function after the illumination is then

$$N'(\omega, x, \Omega) = N^\circ + \Delta N(\omega, x, \Omega), \quad (6)$$

where N° is constant.

After the PSHB procedure is completed, we illuminate the sample with another pulse (probe pulse) of amplitude $s_3(t)$, while, at the same time, we apply a homogeneous electric field \mathbf{E} . The intensity of the probe pulse is taken low enough that it has a negligible effect on the inhomogeneous distribution function. The impurity molecules scatter the probe light resonantly, and because of the grating in the spatial and frequency distribution of the ZPL's, a fraction of the probe amplitude is diffracted in a direc-

where $\alpha_0 = (2\pi)^2 \nu_0 \eta L N^\circ (hc)^{-1}$ and the angle brackets denote integration over the ZPL resonance frequencies ω' as well as over the orientations of the molecules, Ω . We have assumed here a Lorentzian line shape,

$$\Gamma(\omega) = \frac{\pi\Gamma_{\text{hom}}}{\omega^2 + (\pi\Gamma_{\text{hom}})^2}, \quad (9)$$

and have neglected the phonon side band. In Eq. (8) the scattered amplitude is written as a separate term corresponding to the inhomogeneous distribution unaffected by the PSHB process in order to distinguish it from the time response that occurs from the bleached out spectral and spatial grating. The time response is expanded into Taylor series of which only the first two terms (the terms inside the braces) are kept. The exponential factor on the left-hand side of Eq. (8) is later omitted. The next step is to substitute Eqs. (3), (5), and (6) into Eq. (8) to get

$$\begin{aligned} A'(t, x, \mathbf{E}) &= \hat{F}^{-1} \left(\tilde{s}_3(\omega) \left\{ 1 + \alpha_0 \left\langle \frac{(\mathbf{d}\mathbf{n})^4 (|\tilde{s}_1(\omega' - 2\pi\nu_0)|^2 + |\tilde{s}_2(\omega' - 2\pi\nu_0)|^2)}{i[\omega' - \omega + F(\mathbf{E}, \Omega)] + 2\pi\Gamma_{\text{hom}}} \right\rangle \right\} \right) \\ &+ \alpha_0 \hat{F}^{-1} \left\{ \tilde{s}_3(\omega) \left\langle \frac{(\mathbf{d}\mathbf{n})^4 \tilde{s}_1^*(\omega' - 2\pi\nu_0) \tilde{s}_2(\omega' - 2\pi\nu_0) \exp \left[-i\omega' \left(\tau - \frac{x \sin \Phi}{c} \right) \right]}{i[\omega' - \omega + F(\mathbf{E}, \Omega)] + 2\pi\Gamma_{\text{hom}}} \right\rangle \right\} \\ &+ \alpha_0 \hat{F}^{-1} \left\{ \tilde{s}_3(\omega) \left\langle \frac{(\mathbf{d}\mathbf{n})^4 \tilde{s}_2^*(\omega' - 2\pi\nu_0) \tilde{s}_1(\omega' - 2\pi\nu_0) \exp \left[i\omega' \left(\tau - \frac{x \sin \Phi}{c} \right) \right]}{i[\omega' - \omega + F(\mathbf{E}, \Omega)] + 2\pi\Gamma_{\text{hom}}} \right\rangle \right\}. \quad (10) \end{aligned}$$

tion different from the direction of the probe beam. The diffracted beam (PASPE) originates from the coherent su-

The first term on the right-hand side of Eq. (10) corresponds to the light beam that passes through the film

without diffraction, and the second and the third terms correspond to the PASPE signal. After integrating over the variable ω' and evaluating the inverse Fourier transform, we get, for the amplitudes of the echo signals,

$$A_{+1}'(t, x, \mathbf{E}) = \int_{-\infty}^t s_3(t') G(t - t', \mathbf{E}) \exp[2\pi(i\nu_0 - \Gamma_{\text{hom}})(t - t')] \times \int_{-\infty}^{\infty} s_1^*(t'') s_2\left(t'' + t' - t - \tau + \frac{x \sin \Phi}{c}\right) dt' dt'' \times \exp\left[i2\pi\nu_0\left(-\tau + \frac{x \sin \Phi}{c}\right)\right], \quad (11a)$$

$$A_{-1}'(t, x, \mathbf{E}) = \int_{-\infty}^t s_3(t') G(t - t', \mathbf{E}) \exp[2\pi(i\nu_0 - \Gamma_{\text{hom}})(t - t')] \times \int_{-\infty}^{\infty} s_2^*(t'') s_1\left(t'' + t' - t - \tau + \frac{x \sin \Phi}{c}\right) dt' dt'' \times \exp\left[i2\pi\nu_0\left(\tau - \frac{x \sin \Phi}{c}\right)\right], \quad (11b)$$

where we have introduced the function

$$G(t, \mathbf{E}) = \int_{\Omega} (\mathbf{dn})^4 \exp[-iF(\mathbf{E}, \Omega)t] d\Omega. \quad (12)$$

Equation (11a) describes the PASPE propagating in the direction $\mathbf{q}_{+1} = (-\sin \Phi, 0, \cos \Phi)$, which corresponds to the first positive diffraction order. Equation (11b) describes the echo signal diffracted in the direction $\mathbf{q}_{-1} = (\sin \Phi, 0, \cos \Phi)$ and corresponds to the first negative diffraction order. We see that the echo amplitudes are expressed as a convolution of the readout pulse amplitude with the time-domain amplitude response of the hologram. The time response function is, in turn, proportional to the function \mathbf{G} multiplied by the cross-correlation function of the two writing pulses.

Let us assume now that $s_1(t)$ and $s_3(t)$ (reference pulses) are both much shorter than $s_2(t)$ (object pulse). [Equivalently, we may assume that the cross-correlation function of $s_1(t)$ and $s_3(t)$ is zero, with the exception of a sharp peak at time $t = 0$.] In other words, we assume the spectra of the pulses s_1 and s_3 to be much broader than the one from s_2 , and we can approximate the amplitudes of the reference pulses with δ functions. Then Eqs. (11) reduce to

$$A_{+1}' = s_2\left(t - \tau + \frac{x \sin \Phi}{c}\right) \mathbf{G}(t, \mathbf{E}) \times \exp\left[i2\pi\nu_0\left(t - \tau + \frac{x \sin \Phi}{c}\right)\right] \exp(-2\pi\Gamma_{\text{hom}}t), \quad (13a)$$

$$A_{-1}' = s_2^*\left(-t - \tau + \frac{x \sin \Phi}{c}\right) \mathbf{G}(t, \mathbf{E}) \times \exp\left[i2\pi\nu_0\left(t + \tau - \frac{x \sin \Phi}{c}\right)\right] \exp(-2\pi\Gamma_{\text{hom}}t). \quad (13b)$$

We see from these equations that in both diffraction orders the time amplitude of the echo signal is multiplied by the same function \mathbf{G} . This function fully characterizes the average Stark shifts of the ZPL's and is universal in the sense that it depends on the electric properties of the

impurity centers and does not depend on the particular time profile (and spectrum) of the excitation pulses or on the width (and shape) of the homogeneous spectral line. Also, it follows from Eqs. (13) that the external field does not change the causality-related property of the diffraction direction^{24,25}: If the delay between the writing pulses is positive over the cross section of the sample, $\tau > |x_{\text{max}}|c^{-1} \sin \Phi$, then the echo signal in the -1 order is zero, and light is diffracted only into the $+1$ direction. In the opposite case (negative time delay), the diffraction takes place only in the negative order, and the reconstructed object pulse is inverted in time.

Equations (11)–(13) reflect the fact that Stark effect can manifest itself as a modulation of the time profile of PASPE. On the other hand, if the time profile of the object pulse is also a δ function, then the echo amplitude is simply

$$A_{+1}' = \mathbf{G}\left(\tau \pm \frac{x \sin \Phi}{c}, \mathbf{E}\right) \exp\left[-2\pi\Gamma_{\text{hom}}\left(\tau \pm \frac{x \sin \Phi}{c}\right)\right]. \quad (14)$$

In particular, it follows from Eq. (14) that the PASPE amplitude may be nonuniform over the cross section of the beam if the delay between the pulses differs much along the x axis.

Now we turn to the investigation of the first-order Stark effect. The frequency shift depends linearly on the projection of the electric field vector on the direction of the vector difference between the static dipole moment in the ground and the excited electronic states and the Stark shifts is

$$F(\mathbf{E}, \Omega) = \frac{2\pi}{h} |\mathbf{E}| |\Delta\boldsymbol{\mu}_{\text{mol}}| \cos \beta, \quad (15)$$

where β is the above-named angle. In our notation the value of the electric field includes the Lorentz-Lorenz correction factor for local field strength in an isotropic dielectric medium. Below we will assume that the angle between the writing beams is sufficiently small to minimize the spatial nonuniformity of the echo. Let the electric field be applied perpendicular to the (x, y) plane, i.e., perpendicular to the polarization vector of light. First we consider impurity molecules with only an intrinsic dipole moment. In this case the function \mathbf{G} can be evaluated analytically:

$$\begin{aligned} \mathbf{G}(t, \mathbf{E}) &= \int_{\Omega} (\mathbf{dn})^4 \exp[iF(\mathbf{E}, \Omega)t] d\Omega \\ &= \int_0^{2\pi} d\phi \int_0^{2\pi} d\varphi \int_0^{\pi} (\sin \beta) d\beta (\mathbf{dn})^4 \\ &\quad \times \exp\left[i\left(\frac{2\pi}{h} |\mathbf{E}| |\Delta\boldsymbol{\mu}_{\text{mol}}| \cos \beta\right)t\right] \\ &= \int_0^{\pi} [A(\theta) + B(\theta)(\cos^2 \beta) + C(\theta)(\cos^4 \beta)] \\ &\quad \times \cos\left[\frac{2\pi}{h} t |\mathbf{E}| (|\Delta\boldsymbol{\mu}_{\text{mol}}| \cos \beta)\right] (\sin \beta) d\beta \\ &= \frac{2}{D} \{2D[B(\theta)D^2 - 2C(\theta)(6 - D^2)](\cos D) \\ &\quad + [A(\theta)D^4 - B(\theta)D(2 - D^2) \\ &\quad + C(\theta)(24 - 12D^2 + D^4)](\sin D)\}, \quad (16) \end{aligned}$$

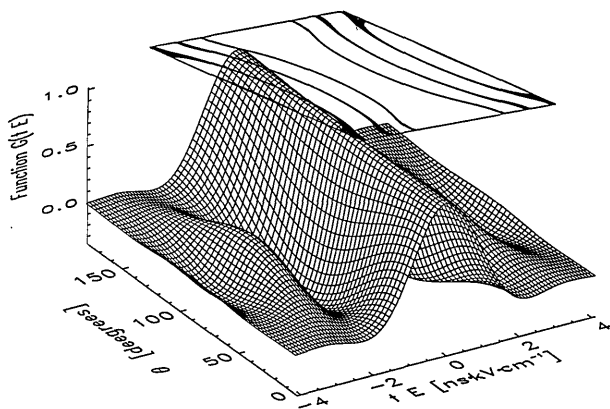


Fig. 2. G calculated (maximum normalized to unity) in the case of linear Stark effect and zero induced dipole moment ($\Delta\mu_{\text{mol}} = 1.0$ D) for different angles between the vectors of the transition dipole moment and the difference of permanent dipole moments ($0 < \theta < 180^\circ$), plotted as a function of the parameter tE . The graph at the top shows the contour of $G = 0$.

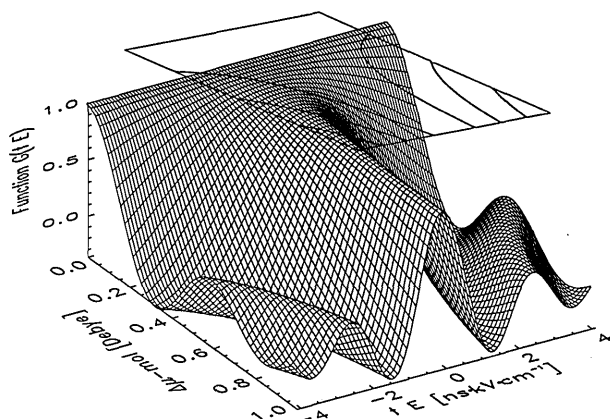


Fig. 3. G calculated as a function of tE depending on $\Delta\mu_{\text{mol}}$ for the case of linear Stark effect and zero induced dipole moment. The angle between the vectors of the transition dipole moment and the permanent dipole moment difference is $\theta = 90^\circ$.

where θ is the angle between the vectors \mathbf{d} and $\Delta\mu_{\text{mol}}$ and $D = (2\pi/h)t|E||\Delta\mu_{\text{mol}}|$. The explicit forms of $A(\theta)$, $B(\theta)$, and $C(\theta)$ are listed in Appendix A. We see that G is a function of a parameter given as $t|E|$. The amplitude of Eq. (14) varies with the electric field for all delay times qualitatively in the same way if the voltage is scaled according to $U' = (t/t')U$. We can also say that the dependence of the PASPE with a fixed time delay between the writing pulses on the applied voltage is given by the same function, as in the case of a fixed voltage and a variable time delay.

Figure 2 shows the function G depending on $t|E|$, calculated according to Eq. (16), for different values of θ ($\Delta\mu_{\text{mol}}$ is taken equal to 1 D). The absolute maximum of G is at $t|E| = 0$. This function has an oscillating character with several local maxima as well as intervals where the function turns negative. The oscillations are most pronounced if the angle θ is close to 90° . Changing the sign of G means switching the phase of the echo amplitude by π . At certain values of $t|E|$ the function G is equal to zero, i.e., the intensity of the PASPE signal [Eq. (14)] is also zero. Such behavior can be interpreted if we consid-

der that in our case Stark shifts occur both in increasing and in decreasing frequency direction (pseudo-Stark splitting). When the absolute frequency shift equals half the grating period, then the two oppositely shifted structures cancel each other, and the grating vanishes. If the Stark shift increases further, then the contrast of the frequency-domain grating is established again but with the phase shifted by half the period.

Figure 3 illustrates how G varies with the magnitude of the permanent dipole moment difference. Here the value of θ is set to 90° . The position of the points where the PASPE signal is zero can serve as an indicator of the magnitude of $|\Delta\mu_{\text{mol}}|$.

In the following calculation, we also take into account the induced dipole moment. This additional dipole moment is caused by the surrounding matrix and is connected to the electric polarizability of the dye molecule.⁵

The static dipole moment difference is given now by the sum of the vectors, $\Delta\mu_{\text{eff}} = \Delta\mu_{\text{mol}} + \Delta\mu_{\text{ind}}$, where $\Delta\mu_{\text{ind}}$ is the difference of the induced dipole moment in the ground and the excited electronic states. We discuss here only molecules with a planar structure, in which case all three vectors $\Delta\mu_{\text{ind}}$, $\Delta\mu_{\text{mol}}$, and \mathbf{d} are in the principal plane of the molecule. We modify Eq. (16) by averaging over the statistical distribution of $|\Delta\mu_{\text{ind}}|$, (around a mean value of $\langle\langle\Delta\mu_{\text{ind}}\rangle\rangle$), and average also over the direction of $\Delta\mu_{\text{ind}}$.

The final expression is

$$G(t|E) = \int_0^{2\pi} d\gamma \int_0^\infty d(|\Delta\mu_{\text{ind}}|) \int_0^\pi (\sin \beta) d\beta P(\beta, \gamma, |\Delta\mu_{\text{ind}}|, \beta) \times \cos[2\pi/h)t|E||\Delta\mu_{\text{eff}}|(\cos \beta)]. \quad (17)$$

The function $P(\theta, \gamma, |\Delta\mu_{\text{ind}}|, \beta)$ is detailed in Appendix A.

Figure 4 shows the result of a numerical integration of Eq. (17). G is plotted for different values of $\langle\Delta\mu_{\text{ind}}\rangle$ and for $\theta = 90^\circ$. We see that the inclusion of the induced dipole moment in our model leads to faster decay of the amplitude with the increasing parameter $t|E|$. At the same time, if the value of $\langle\Delta\mu_{\text{ind}}\rangle/|\Delta\mu_{\text{mol}}|$ is less than approximately 0.5, the position of the zero point is practically not affected. On the other hand, if $\langle\Delta\mu_{\text{ind}}\rangle/|\Delta\mu_{\text{mol}}| > 0.9$, the zero points vanish and the amplitude of the oscillations

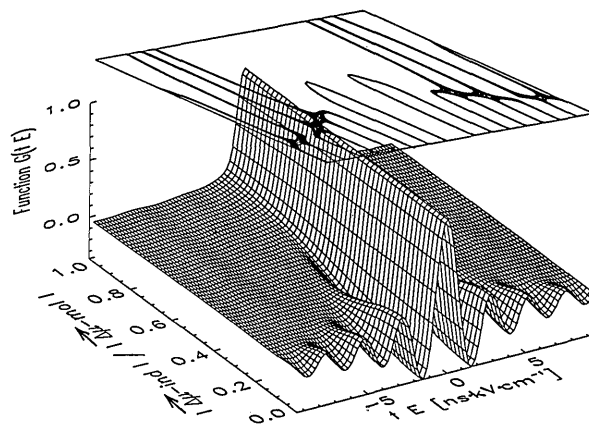


Fig. 4. G calculated as a function of tE for the case of linear Stark effect depending on $\Delta\mu_{\text{ind}}/\Delta\mu_{\text{mol}}$. The angle between the vector of the transition dipole moment and the vector of the intrinsic permanent dipole moment difference is $\theta = 90^\circ$. Contour lines correspond to values $G = 0$.

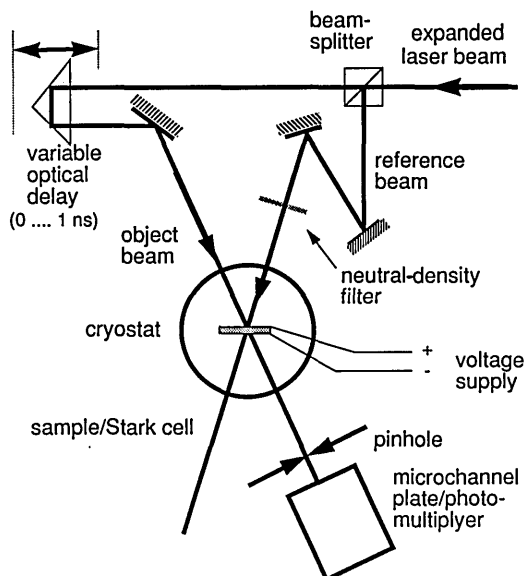


Fig. 5. Experimental setup. The laser beam is expanded in a telescope and divided into a reference and an object beam by a nonpolarizing beam-splitter cube. Both beams are directed by mirrors to the sample with a crossing angle of 10° .

tions becomes smaller. In the limit of $\langle |\Delta\mu_{\text{ind}}| \rangle \gg |\Delta\mu_{\text{mol}}|$ (centrosymmetric molecules), function G has neither zero points nor oscillations and is given by a smooth bell-shaped profile.

EXPERIMENTAL

The experiments were carried out by using a DCM or Rhodamine 6B picosecond dye laser with an average power of 100 mW, synchronously pumped by a mode-locked frequency-doubled Nd:YAG laser (Coherent Antares Model 76s). The duration of the dye laser pulses is a few picoseconds, the spectral width of the pulses is in the frequency domain of 120 GHz, and the repetition rate of the picosecond pulses is 76 MHz.

Our samples were prepared by using the standard procedure of adding dye to a solvent containing dissolved polymer and pressing the polymer film after evaporation of the solvent between two heated glass plates coated with semitransparent electrodes. The strength of the electric field is calculated from the voltage applied to the electrodes (± 1 kV) and from the measured distance between the glass plates (typically 50–150 μm) and by taking into account the Lorentz-Lorenz local field correction factor. The polymer we used was PVB, and it has a dielectric constant of $\epsilon = 2.5$. The experiments were carried out with two different types of sample. In one case the PVB was doped with chlorin molecules; in the other case the polymer contained the molecules of octaethylporphyrin. The concentration of the impurity molecules in both cases was of the order of 10^{-3} mol/L. During the experiments the sample was contained in an optical cryostat immersed in superfluid helium. The temperature was 1.6 K.

The optical scheme of our experiment is shown in Fig. 5. The laser beam is expanded in a telescope and divided into a reference and an object beam by a nonpolarizing beam-splitter cube. Both beams are directed by mirrors to the sample with a crossing angle of 10° . We can vary the delay of the object beam with respect to the reference beam in an interval of 0–1.0 ns.

The intensity in each of the beams during the PSHB procedure is approximately 1–10 mW/cm^2 . To write the hologram, we set the applied voltage to zero and expose our sample to both beams simultaneously for 30 s. After exposure, the object beam is blocked, and the readout reference beam is attenuated with a neutral-density filter.

The time-integrated intensity of the PASPE signal is measured by using a photomultiplier together with a conventional photon-counting system. A time-resolved measurement of the PASPE signal is carried out with a fast microchannel plate photodetector together with a time-correlated signal photon-counting system.²⁶ To reduce the scattered light incident upon the detectors, we focused the PASPE signal through a pinhole.

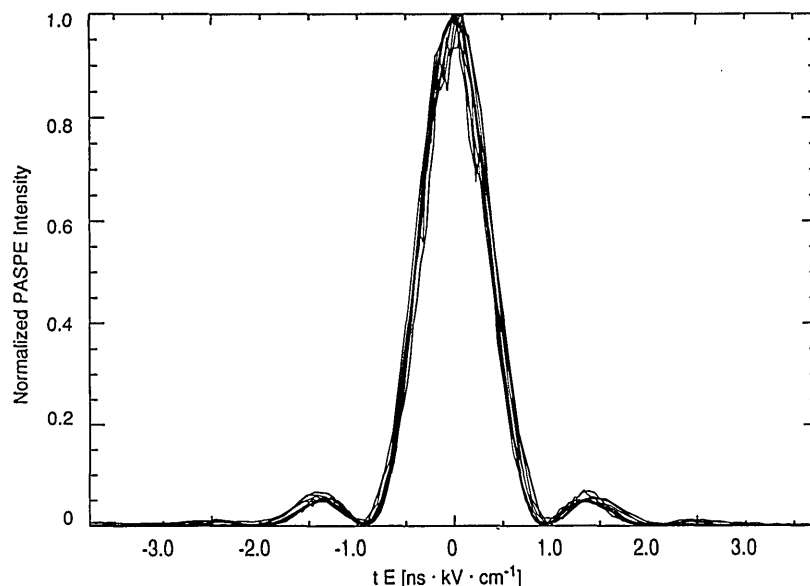


Fig. 6. Intensity of the PASPE signal in chlorin/PVB film at 1.9 K versus the applied electric field. The experimental traces obtained with different delay values between the writing pulses ($9 \text{ ps} < t < 530 \text{ ps}$) are superimposed after scaling to tE and normalizing the signal intensity to unity at the absolute maximum.

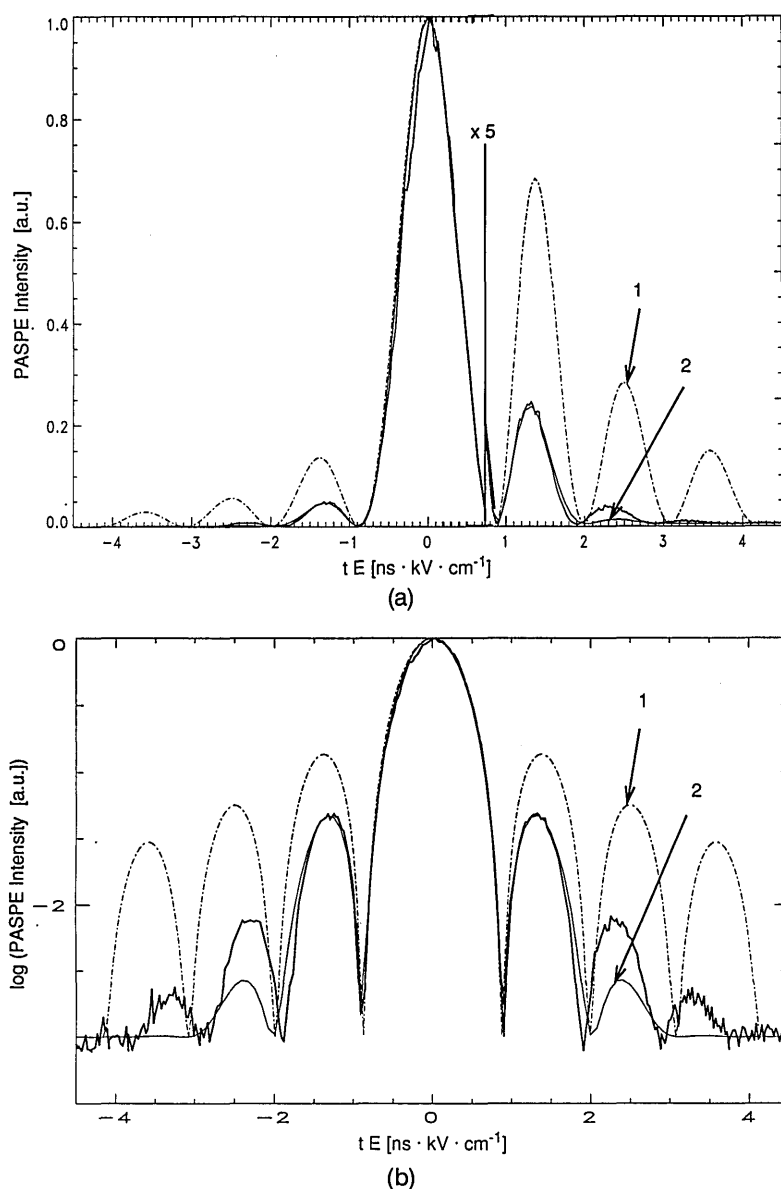


Fig. 7. (a) Electric field dependence of the intensity of PASPE in chlorin/PVB film with a time delay of $t = 390$ ps measured at 1.9 K (bold, solid curve) and two theoretically calculated curves without (dashed curve, 1) and with (solid curve, 2) taking into account the induced dipole moment (see text). The right part of the figure is plotted on an expanded scale (expansion factor, 5). (b) The same data in (a) presented on an intensity logarithm scale.

RESULTS AND DISCUSSION

We perform two types of experiment with our setup. In one case we study the time-integrated intensity of the PASPE depending on the Stark field and on the delay between the writing reference and object pulse. In the second experiment we record a hologram of an object pulse comprising a train of picosecond pulses and study the effect of the applied electric field on the time profile of the PASPE signal.

Our first experiment is to record a trivial time-domain hologram by illuminating the sample with the two writing beams of equal intensity and with the time profile of the pulses corresponding exactly to the output pulses of the dye laser. During exposure, we keep the time delay between the object and the reference beam constant. After exposure is complete, we block the beam that was delayed

and illuminate the sample with only the attenuated beam of the shorter path length. The PASPE signal observed behind the sample is diffracting from the hologram in the direction of the blocked beam. We use a conventional photomultiplier and photon-counting system to detect the intensity of the PASPE signal depending on the voltage applied to the electrodes of the Stark cell. We make several exposures with different values of the time delay between the writing pulses in an interval of 0–600 ps. The different exposures are made at different spatial locations by moving the illuminated spot across the sample or by varying slightly (1 nm) the wavelength in order to find a virgin spectral interval of the inhomogeneous absorption band.

Figure 6 shows the experimentally measured PASPE intensities as a function of the parameter $t|E|$. All traces follow basically the same profile, proving our theoretical

conclusion that in the case of a linear Stark effect the influences of time delay and the electric field strength are reciprocal to each other.

In Fig. 7, one selected experimental trace ($t = 390$ ps, bold, solid curve) is compared with two calculated curves. The first curve (dashed) is calculated according to Eq. (16) and shows a larger modulation amplitude than that observed in the experiment. The second curve (thin, solid) is calculated according to Eq. (17) and differs from the experimental curve by less than 1%. The best fit for the second curve is obtained with the value of the molecular dipole moment difference of 0.28 D and the value of the mean-induced dipole moment difference of 0.084 D. These values are in good agreement with earlier data.⁵ Here the fitting of the experimental data with the calculated curves is simplified compared with that in earlier methods based on narrow spectral holes because we do not need to consider the homogeneous line shape of ZPL's.

Figure 8 shows the result obtained with the impurity molecule octaethylporphyrin. We model the experimental data by a model curve calculated according to Eq. (17), where we set $\Delta\mu_{\text{mol}} = 0$. The best fit is obtained with the mean value of the matrix-induced dipole moment of $\langle|\Delta\mu_{\text{ind}}|\rangle = 0.065$ D. This value is also in reasonable agreement with the previously reported data for the same system ($\Delta\mu_{\text{ind}} = 0.10$ D).⁵ The absence of the permanent dipole moment in the case of centrosymmetric octaethylporphyrin molecules agrees well with the observed smooth dependence of the echo signal on the applied electric field.

Now we turn to the experimental verification of Eqs. (13), which state that changing the strength of the applied electric field modulates the time profile of a temporally extended PASPE signal. In this experiment we use a chlorin sample in a PVB film. To generate an object pulse with an amplitude extending in time longer than the duration of the laser pulses, we take a Fabry-Perot étalon consisting of two highly reflecting flat mirrors and place it into the object beam before the cryostat. The time profile of the object beam reaching the sample now consists of a train of equally spaced pulses with a time delay (120 ps) between two adjacent ones given by

the spacing of the interferometer mirrors. The reference beam is also delayed so that it arrives a few picoseconds earlier than the twelfth pulse of the object pulse train. The readout of the hologram is carried out by illumination with the reference beam. Because the writing reference pulse overlaps in time with the object pulse train, both positive and negative diffraction orders are simultaneously observed during the readout of the hologram. We detect the echo signal in the -1 diffraction order.

Figure 9(a) summarizes the experimental results. The width of individual pulses in the measured intensity profile of the PASPE time-domain hologram is defined by the time resolution of our apparatus (~ 80 ps) rather than by the actual duration of the laser pulses (< 5 ps). The uppermost trace was accumulated at zero voltage, and the curves below are presented in the order of increasing voltage (up to 11.2 kV cm⁻¹) applied during the measurement. As expected, the first PASPE pulse, which corresponds to a delay near zero, exhibits no variation with the electric field. With all other pulses, however, we can observe a dependence on the applied voltage. The effect of the electric field consists of a time-domain oscillating function that is superimposed upon the original PASPE pulse train. The pulses with the largest delay are most sensitive to the applied voltage.

In Fig. 9(b) we present calculated curves that simulate the results of the experiment described above. We assume that the PASPE time-domain hologram in the zero electric field consists of an exponentially decreasing train of δ -shaped pulses. The intensity profile of the pulse train is multiplied by function G^2 , calculated according to Eq. (17), and by taking the values of the Stark parameters found from our previous experiment. The result is then convoluted with the prompt time response function of our time-correlated single-photon-counting apparatus, which is determined in a separate measurement. Good agreement found between Figs. 9(a) and 9(b) can be interpreted as additional proof of our theoretical considerations summarized in Eqs. (13).

Besides the possibility of measuring the Stark effect parameters, our method provides an additional capability to

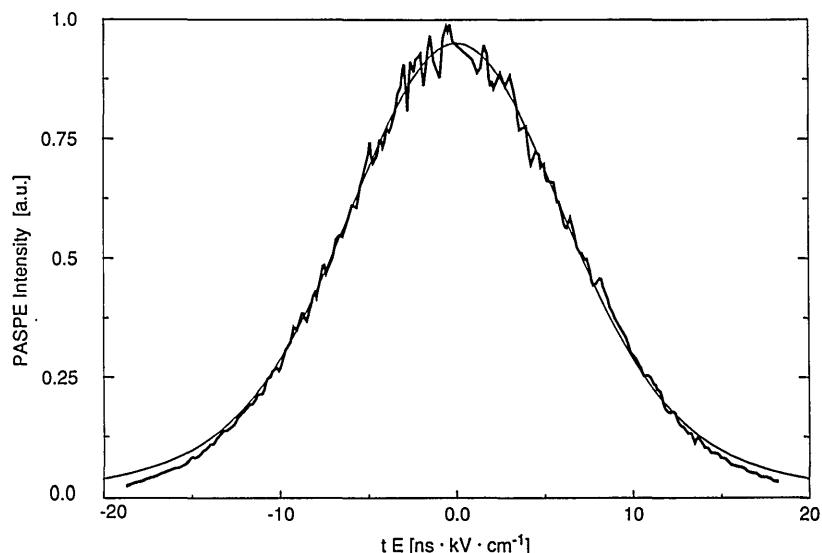


Fig. 8. Electric field dependence of the intensity of PASPE in an octaethylporphyrin/PVB film with a time delay of $t = 390$ ps: experiment, bold, solid curve; calculated, thin curve (see text).

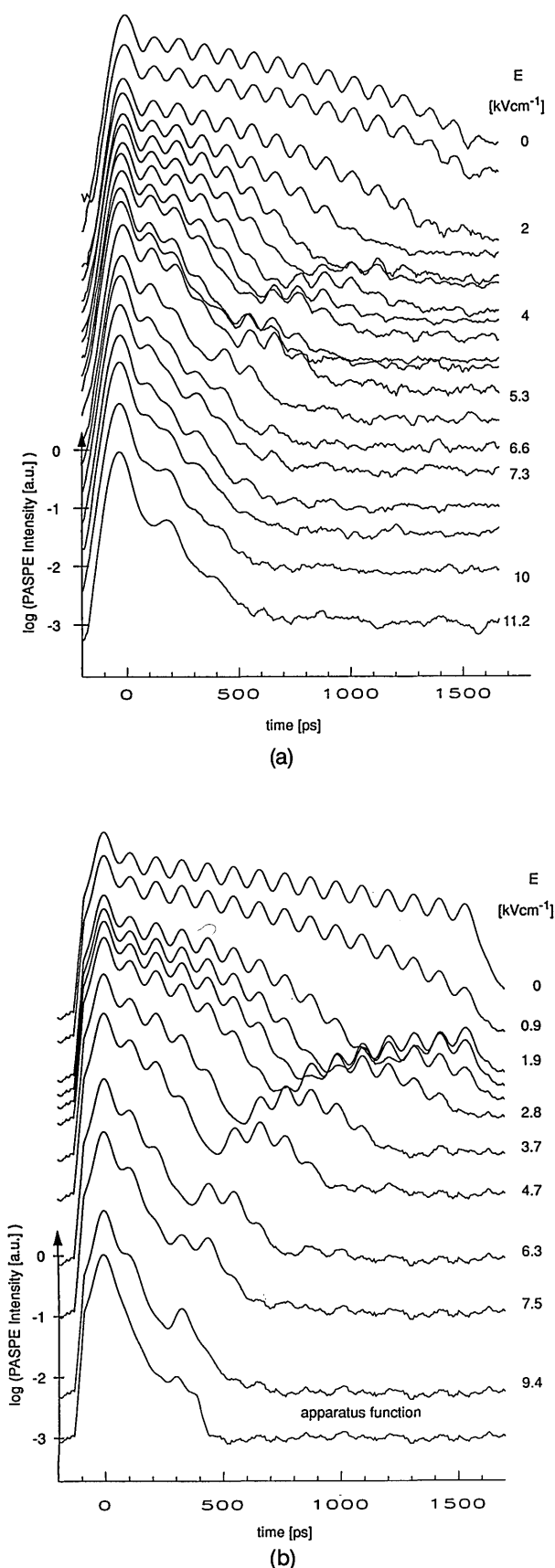


Fig. 9. (a) Time-resolved intensity of PASPE in a chlorin/PVB film at 1.9 K. The uppermost trace is measured at zero electric field; the traces below are shown in order of increasing value of the applied voltage (see text). (b) Simulation of the time-domain PASPE hologram in electric field (see text).

the technique of the time-domain holography. For example, analogous to the electric field domain multiplexing and interference of PSHB holograms,⁵ an applied external field can also be used to manipulate time-domain holograms written at different values of the electric field.

CONCLUSIONS

We have demonstrated a new experiment in which Stark effect manifests itself as the dependence of the intensity of the PASPE on applied electric field. We showed that this dependence can be used to determine the intrinsic and induced dipole moment difference of dye molecules in polymeric matrices at low temperature. We also evaluated theoretically and experimentally the influence of the external electric field on the time-domain holograms stored by means of PSHB.

APPENDIX A

$$A(\theta) = \frac{1}{64}[9 + 6(\cos^2 \theta) + 9(\cos^4 \theta)],$$

$$B(\theta) = \frac{1}{64}[6 + 36(\cos^2 \theta) - 90(\cos^4 \theta)],$$

$$C(\theta) = \frac{1}{64}[9 - 90(\cos^2 \theta) + 105(\cos^4 \theta)], \quad (\text{A1})$$

$$P(\theta_{\text{eff}}, \gamma, |\Delta\mu_{\text{ind}}|, \beta) = [A(\theta_{\text{eff}}) + B(\theta_{\text{eff}})(\cos^2 \beta) + C(\theta_{\text{eff}})(\cos^4 \beta)]|\Delta\mu_{\text{ind}}| \times \exp\left(-\frac{|\Delta\mu_{\text{ind}}|^2}{\langle|\Delta\mu_{\text{ind}}|^2\rangle}\right), \quad (\text{A2})$$

$$\theta_{\text{eff}} = \theta - \alpha \sin\left(\frac{|\Delta\mu_{\text{ind}}|}{|\Delta\mu_{\text{eff}}|}\right)(\sin \gamma), \quad (\text{A3})$$

$$|\Delta\mu_{\text{eff}}| = (|\Delta\mu_{\text{mol}}|^2 + |\Delta\mu_{\text{ind}}|^2 + 2|\Delta\mu_{\text{mol}}||\Delta\mu_{\text{ind}}|\cos \gamma)^{1/2}. \quad (\text{A4})$$

ACKNOWLEDGMENTS

We thank Alois Renn for help in calculating the induced dipole moment and Ekkehard Görlach for participating in the experiments. We thank Guido Grassi and Petra Kohler for synthesizing chlorin. This research was supported by the Swiss National Science Foundation.

REFERENCES

1. K. K. Rebane, *Impurity Spectra of Solids* (Plenum, New York, 1970).
2. O. Sild and K. Haller, *Zero Phonon Lines* (Springer-Verlag, Berlin, 1988).
3. A. A. Gorokhovskii, R. K. Kaarli, and L. A. Rebane, *JETP Lett.* **20**, 216 (1974).
4. B. M. Kharlamov, R. I. Personov, and L. A. Bykovskaya, *Opt. Commun.* **12**, 191 (1974).
5. A. J. Meixner, A. Renn, S. E. Bucher, and U. P. Wild, *J. Phys. Chem.* **90**, 6777 (1986).
6. F. A. Burkhalter, G. W. Suter, U. P. Wild, V. D. Samoilenko, N. V. Razumov, and R. I. Personov, *Chem. Phys. Lett.* **94**, 483 (1983).
7. L. Kador, D. Haarer, and R. I. Personov, *J. Chem. Phys.* **86**, 5300 (1987).

8. A. Renn, A. J. Meixner, U. P. Wild, and F. A. Burkhalter, *Chem. Phys.* **93**, 157 (1985).
9. A. J. Meixner, A. Renn, and U. P. Wild, *J. Chem. Phys.* **93**, 6728 (1989).
10. D. A. Wiersma, in *Advances in Chemical Physics XLVII*, J. Jortner, R. D. Levine, and S. A. Rice, eds. (Wiley, New York, 1981), p. 421.
11. A. Rebane, R. Kaarli, P. Saari, A. Anijalg, and K. Timpmann, *Opt. Commun.* **47**, 173 (1983).
12. A. Rebane and D. Haarer, *Opt. Commun.* **70**, 478 (1989).
13. A. K. Rebane, R. K. Kaarli, and P. M. Saari, *Opt. Spectrosc. (USSR)* **55**, 238 (1983).
14. V. V. Samartsev and R. G. Usmanov, *Phys. Stat. Solidi* **49**, 789 (1978).
15. T. W. Mossberg, R. Kachru, S. R. Hartmann, and A. M. Flusberg, *Phys. Rev. A* **20**, 1976 (1979).
16. W. Hesselink and D. A. Weirsma, *J. Chem. Phys.* **75**, 4192 (1981).
17. M. D. Crisp, *Phys. Rev. A* **1**, 1604 (1970).
18. P. Saari, R. Kaarli, and A. Rebane, *J. Opt. Soc. Am. B* **3**, 527 (1986).
19. A. Rebane and O. Ollikainen, *Opt. Commun.* **83**, 246 (1991).
20. H. Gygax, E. Görlach, A. Rebane, and U. P. Wild, *J. Lumin.* **53**, 59 (1992).
21. Y. P. Wang and R. S. Meltzer, *Phys. Rev. B* **45**, 10119 (1992).
22. A. J. Meixner, C. M. Jefferson, and R. M. Macfarlane, *Phys. Rev. B* **46**, 5912 (1992).
23. J. H. Eberly, S. R. Hartmann, and A. Szabo, *Phys. Rev. A* **23**, 2502 (1981).
24. P. Saari and A. Rebane, *Proc. Estonian Acad. Sci. Phys. Math.* **31**, 32 (1984).
25. A. Rebane, S. Bernet, A. Renn, and U. P. Wild, *Opt. Commun.* **86**, 7 (1991).
26. U. P. Wild, A. R. Holzwarth, and H. P. Good, *Rev. Sci. Instrum.* **48**, 1621 (1977).